International Journal of Nanomedicine

Dovepress
Taylor & Francis Group

Open Access Full Text Article

ORIGINAL RESEARCH

Stem Cell-Derived Exosomes with High Expression of PD-L1 as Nanotherapeutics in Rheumatoid Arthritis Model Mice

Siyi Wang[1], Keqin Zhang[2], Li Wang[1], Yuehua Guo[3]

[1]Department of Rheumatology, Kunshan Hospital of Traditional Chinese Medicine, Suzhou, 215300, People's Republic of China; [2]Department of Endocrinology, Tongji Hospital Affiliated to Tongji University, Shanghai, 200065, People's Republic of China; [3]Research Center of Clinical Medicine, Affiliated Hospital of Nantong University, Nantong, 226001, People's Republic of China

Correspondence: Li Wang, Kunshan Hospital of Traditional Chinese Medicine, Suzhou, 215300, People's Republic of China, Email 77934126@qq.com; Yuehua Guo, Research Center of Clinical Medicine, Affiliated Hospital of Nantong University, Nantong, 226001, People's Republic of China, Email guoyuehuanju@163.com

Purpose: Previous studies have identified synovial T cells as key pathogenic drivers of rheumatoid arthritis (RA). To explore a novel therapeutic strategy targeting these cells, we aimed to develop mesenchymal stem cell-derived exosomes with enhanced PD-L1 expression (Exo-PD-L1) and evaluate their therapeutic potential in RA.

Methods: Mouse bone marrow mesenchymal stem cells (MSCs) were stimulated with interferon γ (IFN-γ) to upregulate programmed death ligand 1 (PD-L1) expression. Exo-PD-L1 was isolated and administered to collagen-induced arthritis (CIA) model mice. Therapeutic effects were assessed through T cell activity assays, in vivo biodistribution tracking, clinical symptom scoring, and histopathological analysis of extremities and major organs.

Results: Exo-PD-L1 significantly inhibited the activity of cultured T cells, was highly concentrated in the joints of RA mice, and significantly improved RA manifestations and histological abnormalities in the extremities of mice. No histological abnormalities were observed in the main organs of the mice.

Conclusion: Exo-PD-L1 can be homed to inflammatory lesions and have the potential to treat RA.

Keywords: rheumatoid arthritis, mesenchymal stem cell, exosome, T cell, treatment

Introduction

RA is a common chronic autoimmune inflammatory disease that leads to the persistent destruction of multiple joints.[1] The global prevalence of RA is approximately 1%, and there is currently no effective cure. In order to relieve joint pain, improve joint function and reduce complications, the patients must consistently use anti-rheumatic drugs, including the following four categories: anti-rheumatic drugs (Disease-modifying anti-rheumatic drugs, DMARDs), glucocorticoids, non-steroidal anti-inflammatory drugs (NSAIDs) and biological drugs.[2,3] Despite significant progress in the clinical treatment of RA over the years, the results remain unsatisfactory because the current treatment aims to inhibit the inflammatory process, for example, by inhibiting the production of inflammatory cytokines or removing inflammatory cells at the site of inflammation.[4–6] Despite the remarkable effects of these treatments, more than 30% of patients with RA still show an inadequate response to first-line treatment.[7] These drugs may have the following disadvantages: (1) less accumulation in inflamed joints, resulting in unsatisfactory efficacy; (2) severe adverse reactions; (3) poor bioavailability, excessive dosage and time of drug administration, and drug enrichment in organs will produce strong side effects.[8] Therefore, there is an urgent need to develop novel therapeutic strategies that not only enhance RA treatment efficacy but also minimize systemic adverse effects. To address this dual challenge, we propose a targeted delivery system designed for preferential accumulation in inflamed joints, leveraging the natural tropism of mesenchymal stem cell-derived exosomes to achieve localized immunomodulation while reducing off-target toxicity.

Received: 4 March 2025
Accepted: 6 July 2025
Published: 11 July 2025

T cells play an important role in the progression of RA.[9] In the pathogenesis of RA, a variety of cytokines are released from T cells, such as tumor necrosis factor-α (TNF-α) and IFN-γ, which trigger the inflammatory response; they can stimulate B cells to produce autoantibodies which damage the joint tissue. Therefore, regulating the activity of T cell is the key to the treatment of rheumatoid arthritis.[10]

PD-L1 and its receptor programmed death-1 (PD-1) are pivotal immune checkpoint regulators that suppress T-cell activation, maintaining immune homeostasis and preventing autoimmune hyperactivation.[11] While systemic enhancement of PD-L1 expression could theoretically alleviate RA by forming PD-1/PD-L1 complexes to dampen inflammation, its broad physiological effects and the difficulty in achieving local joint targeting limit their therapeutic utility. MSCs express PD-L1 and exhibit tropism to inflammatory sites (also known as homing ability)[12,13] because the cells can be attracted by chemical factors expressed at inflammatory sites. However, the systemic application of MSCs has the following disadvantages: (1) MSCs selectively accumulate in the lung and liver and insufficiently reach the targeted sites; (2) most of the infused MSCs are captured by macrophages in the liver, spleen, and lung; and (3) the survival and migration ability of infused MSCs in vivo is not as good as that in the in vitro study. These limitations underscore the need for cell-free alternatives. MSC-derived exosomes have emerged as promising therapeutic vectors. Unlike whole MSCs or genetically modified variants which carry tumorigenic risks, exosomes retain parental MSCs homing molecules while eliminating genomic material and immunogenicity. Critically, their bioactive cargo (miRNAs, cytokines) enables multimodal RA intervention by: (1) anti-inflammatory effects: they can reduce the levels of inflammatory mediators, such as TNF-α, IL-1β, and IL-6, thereby inhibiting the inflammatory response;[14] (2) immunomodulatory effects: some components of exosomes can regulate the function of T cells, B cells, and monocytes. In this study, bone marrow-derived MSCs were isolated from mice and subsequently stimulated with IFN-γ to induce high expression of PD-L1. Exo-PD-L1 were successfully isolated through ultracentrifugation. Upon co-culture with T cells for 24 hours, Exo-PD-L1 was observed to be internalized by T cells, resulting in significant suppression of their proliferative capacity. This inhibitory effect was mechanistically attributed to PD-L1/PD-1 binding, which was found to block T-cell activation and reduce the secretion of pro-inflammatory cytokines, including TNF-α and IFN-γ. Following intravenous administration into CIA mouse models, targeted accumulation of Exo-PD-L1 in inflamed synovial joints was confirmed via in vivo imaging. Pathological features such as synovial hyperplasia, angiogenesis, and inflammation were markedly alleviated in Exo-PD-L1-treated groups compared to controls, ultimately demonstrating therapeutic efficacy against RA (Scheme 1). Based on this rationale, our study aimed to investigate whether EXO-PD-L1 can accumulate in inflamed joints and serve as a new treatment approach for RA.

Materials and Methods

Cell Lines

Jurkat cells were purchased from the American Classic Cell Culture Collection (ATCC). T cells were resuspended in RPMI-1640 basal medium at 1×10^6 cells per dish and placed in an incubator for approximately 7 days to harvest the cells.[15] BALB/C mice with bone marrow-derived MSCs were used for primary cell extraction. After the mice were sacrificed and disinfected, the tibia, fibula, and femur were cut off using scissors, and the attached muscle or connective tissue was removed. These bones were placed in 75% ethanol for 5 min and then transferred to Hanks' solution to wash off surface alcohol. The bone marrow cavity was flushed repeatedly with a syringe until the surface of the leg bones turned from red to white, the cell mass was blown repeatedly with a pipette to be dispersed, filtered through a 70 μm cell filter, transferred to a centrifuge tube, centrifuged at 1500 rpm for 5 min, the supernatant was discarded, the cells were resuspended with 2 mL of red blood cell lysate and left for lysis for 5 min, then centrifuged at 1500 rpm for 5 min, and the supernatant was discarded. The cells were resuspended in DMEM complete medium containing 0.1%MCSF and harvested every seven days in an incubator.[16]

Characterization of MSC

The collected cells were centrifuged at 300 × g for 5 min, and the precipitate was retained, washed twice with pre-cooled PBS containing 1% FBS, and the cells were dispersed with 400 μL staining buffer solution (Biolegend), Anti-CD29/PE

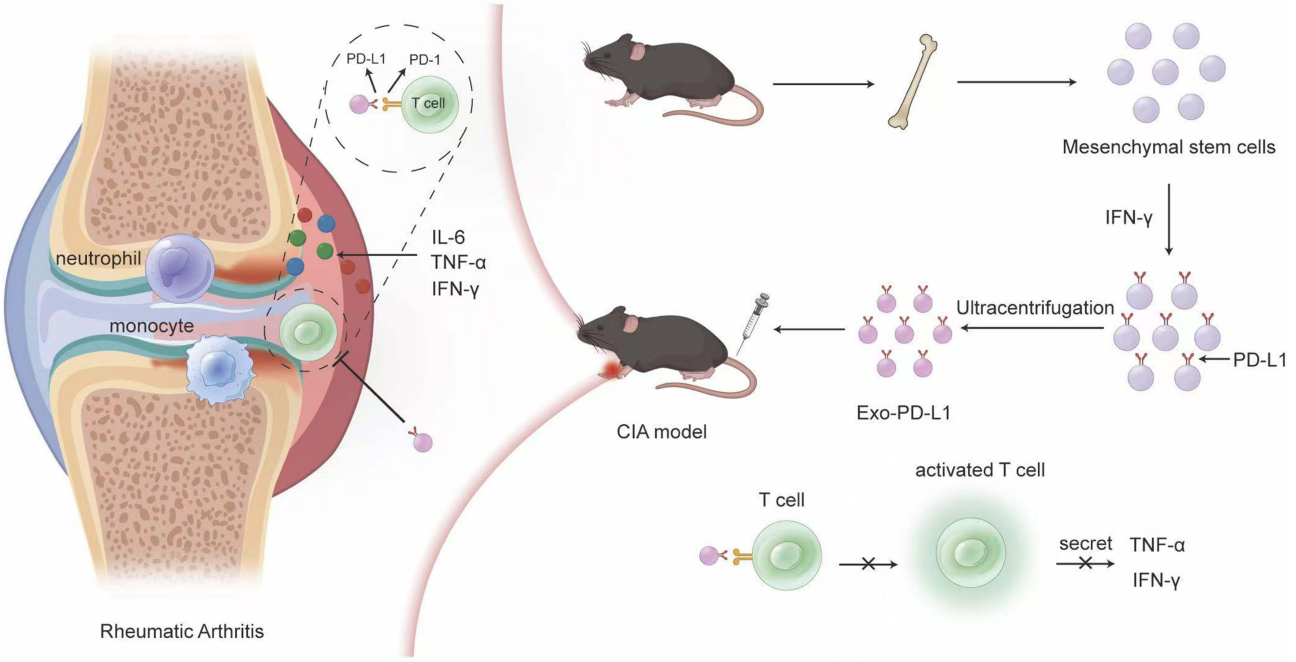

Scheme 1 Schematic illustration. IFN-γ stimulation induces PD-L1 upregulation on MSCs, followed by isolation of Exo-PD-L1, which are intravenously administered via tail vein injection to CIA model mice for targeted RA treatment.

antibody was added, IC fixative was added after the reaction. Anti-CD90/APC antibody was added, and the supernatant was discarded and resuspended for analysis by flow cytometry.

The cells were spread in 24-well plates, washed twice with PBS, and fixed with 4% paraformaldehyde for 30 min. The fixative was then washed and permeabilized with 0.5% Triton X-100 for 15 min. The cells were blocked with 5% bovine serum albumin (BSA) for 1 h. The diluted Anti-CD105 antibody [EPR19911-220], Anti-CD90/Thy1 antibody [EPR3132], Anti-CD44 antibody [F10-44-2] and Anti-CD11b antibody [EPR1344] with fluorescence were dropped onto small discs loaded with cells. The cells were incubated overnight at 4 °C in the dark. On the second day, the cells were warmed for 30 min, washed three times with PBS, stained with DAPI dye for 15 min, covered with an anti-fluorescence quenching sealant drop, and imaged under a fluorescence microscope.[12]

Isolation of Exosomes Expression with PD-L1

MSCs were first stimulated with different concentrations of IFN-γ (0, 0.1, 1, 10, and 100 ng/mL) for 24 h, and then cultured in serum-free DMEM for 24 h. The supernatant was collected and centrifuged at 300 × g for 5 min, 1000 × g for 10 min, 16500 × g for 30 min, and 150000 g for 2 h. The precipitate was suspended in 200 μL of PBS and stored at −80 °C until further use.

Characterization of Exosomes

The morphology of the exosomes was analyzed by transmission electron microscopy (TEM, Talos, USA). Ten microliters of the exosome suspension was dropped on the surface of the copper mesh, after which the tungsten phosphate compound solution was dropped on the surface of the copper mesh and then placed in the TEM (Talos, USA) for photographing.[12] Exosomes were identified by Western blot (WB). Proteins from MSC-Exo, Exo-PD-L1, and MSCs were extracted using RIPA lysis buffer and their concentrations were measured using a BCA assay kit. Proteins were denatured and separated by sodium dodecyl sulfate-polyacrylamide gel electrophoresis. Next, the proteins were transferred onto polyvinylidene fluoride (PVDF) membranes, which were blocked with 5% nonfat powdered milk. Following incubation with Anti-CD9 antibody [Abcam] and Anti-CD63 antibody [Abcam] for 12 h, the membranes were incubated with HRP-conjugated mouse anti-rabbit secondary antibody for 2 h. Finally, the chemiluminescent substrate was dropped onto the membranes,

https://doi.org/10.2147/IJN.S522245

which were then imaged using a Gel Doc XR system (Bio-Rad Laboratories Inc., Hercules, CA, USA). The distribution of exosomes was measured using a nanoparticle tracking analyzer (NTA, ZetaView 120).

Identification of PD-L1 Expressed on Exosomes Under IFN-γ Stimulation

MSCs were stimulated with IFN-γ at concentrations of 0, 0.1, 1, 10, and 100 ng/mL for 24 hours. The MSCs, spread in 24-well plates, washed twice with PBS, and fixed with 4% paraformaldehyde for 30 min. The fixative was then washed and permeabilized with 0.5% Triton X-100 for 15 min. The cells were blocked with 5% bovine serum albumin (BSA) for 1 h. The diluted Anti-PD-L1 antibody (Abcam, Cambridge, UK) was dropped onto small discs loaded with cells and incubated overnight at 4 °C. After 30 min of rewarming, the cells were washed 3 times with PBS, incubated with GFP secondary antibody in the dark for 1h, stained with DAPI dye for 15 min, and anti-fluorescence quench sealing agent was dropped after washing, and images were taken under a fluorescence microscope.[12] qRT-PCR was performed to measure PD-L1 expression. Firstly, l mL of Trizol was added and the reaction was performed at 4 °C for 30 min. Then, 200 μL trichloromethane (CCl_3) was added for 10 min. After centrifugation at 12000 rpm for 15 min at 4 °C, the supernatant was discarded, and 400 μL of isopropanol was added for 10 min, followed by centrifugation at 12000 rpm for 10 min, the supernatant was discarded. After centrifugation, 1 mL of ethanol was added to the pellet, which was then dried and resuspended in DEPC water. RNA was reverse-transcribed into complementary DNA (cDNA) using HiScript III RT SuperMix for qPCR (+gDNA wiper) (Vazyme, China) with a T100TM Thermal Cycler (BIO-RAD), and then quantified by qPCR using 2× SYBR Green qPCR Mix (ES Science, China) with LightCycler® 96 (Roche). All processes were performed according to the manufacturer's instructions. The relative changes in gene expression were identified using the 2−ΔΔCt method. Finally, the expression of PD-L1 in exosomes was measured with WB.

CCK8 Assay to Verify the Inhibitory Effect of Exo-PD-L1 on Jurkat T Cell Activity

The cell density was adjusted to 5×10^4 cells/mL and seeded into 96-well plates at a volume of 100 μL per well, and the plates were placed in an incubator. CCK8 working solution was added 24, 48, 72, and 96 h after the cells were seeded, and the cells were incubated at 37 °C for 2 h. The absorbance was measured using a microplate reader.

ELISA for Measuring Inflammatory Factors

0.1 mL of the test sample was added to the reaction well and incubated at 37 °C for 1 h. Enzyme-labeled antibodies (0.1 mL) were added and incubated at 37 °C for 0.5h, followed by washing. TMB substrate solution (0.1 mL) was added and incubated at 37 °C for 30 min. 0.05 mL of a 2 M termination solution was added. The OD density of each well was measured at 450 nm wavelength using a microplate reader. Levels of TNF-α and IFN-γ were tested with Mouse TNF-α ELISA Kit (ab208348, Abcam) and Mouse IFN-γ ELISA Kit (ab282874, Abcam).

Fluorescence Microscopy for Observing Exosome Uptake by T Cells

Cy5 (CM17830, Proteintech) was used to label the exosomes. 5 μL of Cy5 dye was added to 150 μL of the exosome solution (200 μg). The mixture was incubated for 30 min at room temperature in the dark and excess dye was removed by ultrafiltration. T cells were seeded in 24-well plates at a density of 5×10^4 cells/well and were cultured for 24 h. The protein concentration of Exosomes were added at a final concentration of 50 μg/mL per well and cultured for 4 h. Finally, DAPI was added and incubated for 30 min. Finally, cells were fixed with 4%PFA for 30 min and photographed using a fluorescence microscope.

Establishment and Treatment of Collagen Induced Arthritis (CIA) Model

DBA/1 mice were randomly divided into four groups: control, saline, Exo, and Exo-PD-L1. Bovine type II collagen was mixed in equal proportions with complete Freund's adjuvant at a final concentration of 1 mg/mL. The emulsion was formed by repeated mixing on ice until it was not dispersed on the water surface. Each mouse was injected subcutaneously at the base of the tail with 0.1 mL of the emulsion. One week later, mice were immunized with a freshly prepared emulsion. After the CIA model was established, the mice were injected from the tail vein with saline, Exo, or EXO-PD-

L1 once a week for three weeks. The Saline group was injected with 0.1 mL saline, the Exo group was injected with 0.1 mL of 10 μg/mL Exo, and the EXO-PD-L1 group was injected with 0.1 mL of 10 μg/mL EXO-PD-L1. CIA severity in the mouse model was scored according to the following criteria: Score 0, no symptoms; Score 1, single toe red and swollen; Score 2, more than one toe red and swollen; Score 3, stiff toes; Score 4, deformity or ankle involvement. The scores of the four paws were summed to obtain a total score.[17] All animal experiments were approved by Affiliated Hospital of Nantong University and conducted per the requirements of the Animal Care and Use Committee (Approval NO. S20240927-002).

Preparation of Tissue Paraffin Sections

The tissues were fixed with PFA, decalcified with EDTA, dehydrated with ethanol, and embedded in paraffin blocks. Tissues were attached to a microtome, sliced, and dried naturally. A longitudinal section of the knee joint was created.

H&E Staining

After decalcification and hydration of the tissue, it was stained with hematoxylin dye for 10 minutes, washed with ddH2O for 1 minute, separated by HCl-ethanol for 10 seconds, rinsed with tap water for 1 hour, washed with distilled water for 1 minute, placed in a gradient of ethanol for 5 minutes, stained with alcohol-eosin staining solution for 5 minutes; the gradient of ethanol from low to high and xylene were each treated for 5 minutes for dehydration and transparency; finally, neutral resin was added and sealed.

Immunohistochemistry

After deparaffinization, hydration, and retrieval, slices were blocked with serum for 30 min. Rabbit anti-TNF-α [EPR19147] and Anti-IL-1β antibody [RM1009] antibodies were added for 12 h and washed three times with PBS. Biotinylated sheep anti-rabbit secondary antibody was added for 1 h and the cells were washed three times with PBS. DAB solution was used for color development, counterstained with hematoxylin solution for 30s, and washed with tap water for 15 min to return to blue. The slices were dehydrated with gradient concentrations of ethanol, made transparent twice with xylene, and sealed with neutral gum.

Micro-Computed Tomography (Micro-CT)

The mice were sacrificed, excess soft tissue was removed, and the distal tibia, ankle joint, and hind limb paw were retained and fixed in 4% PFA. Micro-CT (Bruker, Germany) was used to scan at a resolution of 5 μm, and 3D reconstruction of the joint was performed to assess the status of the osteoclast.[12]

Statistical Processing

All data were analyzed using GraphPad Prism software (version 5.0; GraphPad Software). Quantitative data conforming to a normal distribution were expressed as ±SD, and quantitative normal data between groups were analyzed using the *t*-test. In this study, the α value was set at 0.05 as the test level, and all *P* values were two-sided probability. Statistical significance was set at $P< 0.05$.

Results

Identification of MSC

Mouse bone marrow-derived MSCs were collected and cultured in Dulbecco's modified DMEM medium containing F12. The expression markers of MSCs, such as CD44, CD105, CD29, and CD90, were detectable, whereas the hematopoietic markers CD34 and CD45 were not expressed. Through flow cytometry (Figure 1A and B), it was observed that 96.5% of the extracted cells were $CD90^+$ and $CD29^+$, while MSC-negative markers, such as CD45 and CD34, were hardly expressed. This indicates that we successfully cultivated double-positive CD90 and CD29 MSCs. Further verification was conducted by immunofluorescence (Figure 1C), revealing that the expression of CD11b and CD45 in the extracted cells was extremely low, while specific MSCs markers, such as CD44 and CD105, were positive.

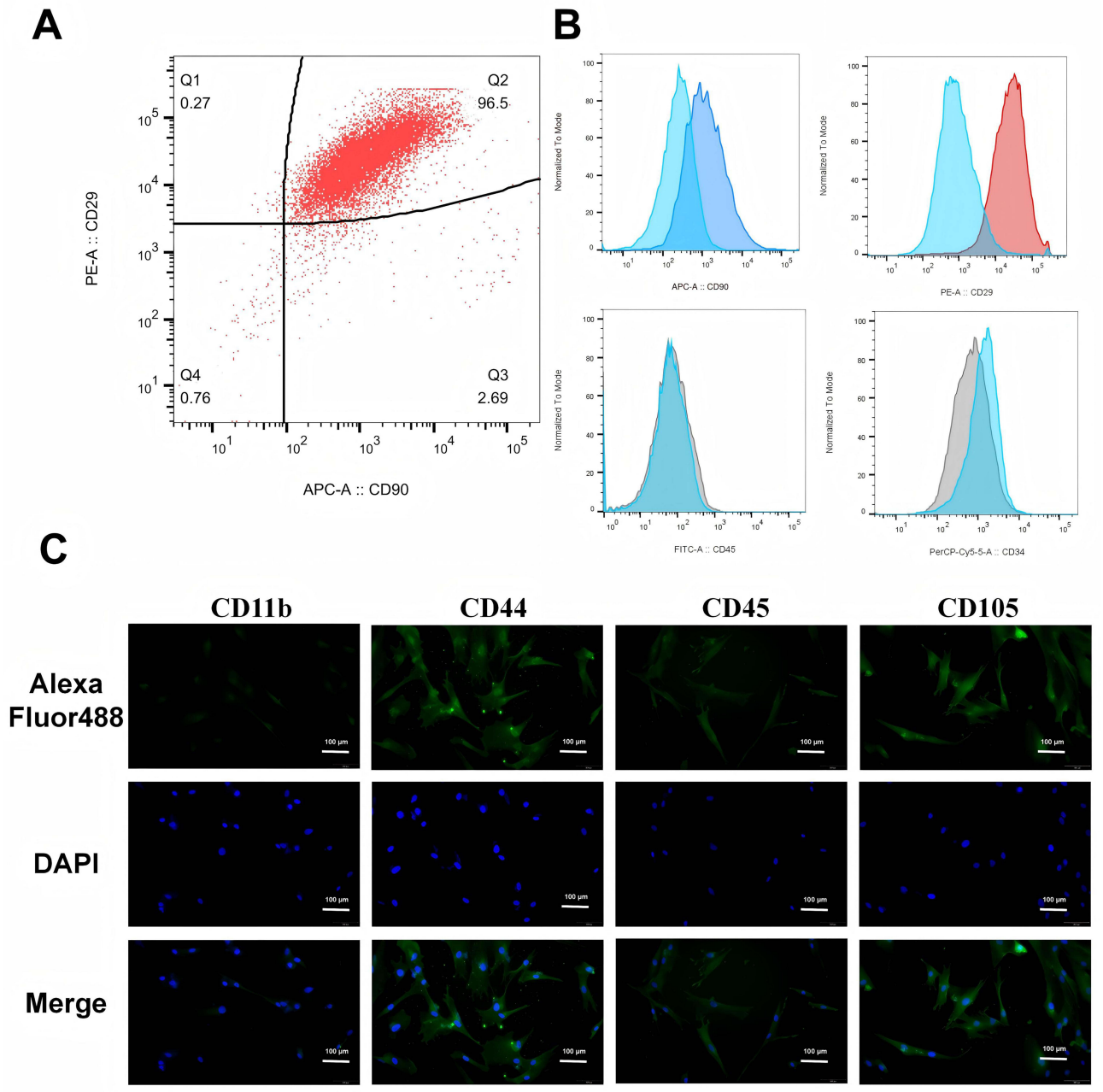

Figure 1 Characterization of MSC. (**A** and **B**) Flow cytometric analysis of MSCs reveals the expression of CD90 and CD29 in MSCs; (**C**) Cellular immunofluorescence of MSCs indicates positive expression of CD44 and CD105, and negative expression of CD11b and CD45. (Green fluorescence is GFP, and blue fluorescence is DAPI.).

Effect of IFN-γ on PD-L1 Expression on MSC Surface

To determine the optimal concentration of IFN-γ for high PD-L1 expression, MSCs were stimulated with five different concentrations of IFN-γ (0, 0.1, 1, 10, and 100 ng/mL) for 24 h. The expression of PD-L1 on MSCs exosomes was validated by immunofluorescence (Figure 2A), qRT-PCR (Figure 2B). As shown in Figure 2A, the expression of PD-L1 gradually increased with increasing concentrations of IFN-γ and peaked at 10ng/mL and 100 ng/mL. This indicated that IFN-γ can stimulate the expression of PD-L1 in MSCs. The PD-L1 mRNA expression results were similar to those obtained by immunofluorescence (Figure 2B). These results indicated that MSCs with high PD-L1 expression were successfully constructed.

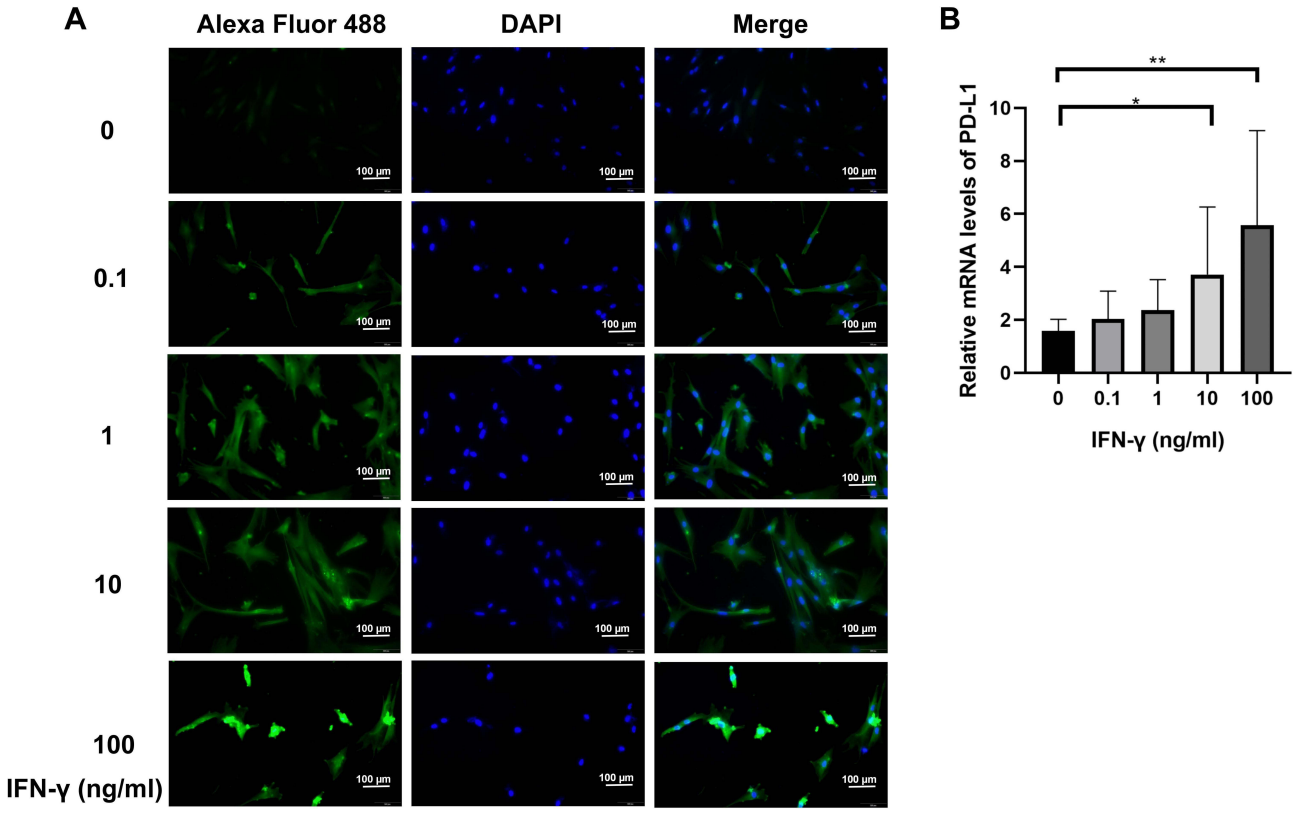

Figure 2 The effect of IFN-γ on PD-L1 expression on the MSC Surface. MSCs were stimulated with IFN-γ at concentrations of 0, 0.1, 1, 10 and 100 ng/mL, and the expression level of PD-L1 was detected by cellular immunofluorescence (**A**) and qRT-PCR (**B**). **P*<0.05, ***P*<0.01 vs control.

Validation of Exosomes

The results revealed that exosomes had a homogeneous spherical structure with a particle size of approximately 150 nm (Figure 3A). NTA results indicated that the diameters of exosomes were mainly distributed within the range of 100–150 nm (Figure 3B). Western Blot analysis showed that the marker proteins CD9 and CD63 in the exosomes were positive (Figure 3C). The above experiments demonstrated that MSC-derived exosomes can be successfully extracted. As for WB, it was observed that the higher the expression of PD-L1 on the surface of MSCs, the higher the expression of PD-L1 in exosomes obtained by ultracentrifugation. As the expression of PD-L1 was significantly different when stimulated with 100ng/mL IFN-γ, the concentration of IFN-γ was 100ng/mL in the subsequent study, indicating that we successfully constructed Exo-PD-L1. We used IFN-γ stimulated MSC-derived exosomes at a concentration of 100 ng/mL, and the resulting PD-L1 was 3.5 times that of the unstimulated counterpart (Figure 3D).

Effect of Exo-PD-L1 on T-Cell Activity

First, we co-cultured Exo-PD-L1 with T cells, and exosomes from MSCs were used as control. As shown in Figure 4A, T cells were able to phagocytose exosomes, and the uptake of Exo-PD-L1 by T cells was higher than that by the Exo group. Next, we stimulated T cells with different concentrations of Exo-PD-L1 and Exo. The CCK-8 assay showed that compared with the blank group, both the Exo-PD-L1 and Exo groups could inhibit the activity of T cells. At the same concentration, the Exo-PD-L1 group showed a better inhibitory effect on T cell activity. With the increase of EXO-PD-L1 concentration and culture time, the inhibitory effect of EXO-PD-L1 on T cells gradually increased.[18] (Figure 4B). Finally, the supernatant was extracted after 4 h of coculture. ELISA showed that the expression of the pro-inflammatory factors TNF-α and IFN-γ decreased with an increase in the concentration of exosomes. Under the same conditions, the inhibitory effect of Exo-PD-L1 on inflammatory factors was greater than that in the Exo group. Moreover, T cells were stimulated with 1×10^7 particles/mL Exo-PD-L1 showed the strongest inhibitory effect on

https://doi.org/10.2147/IJN.S522245

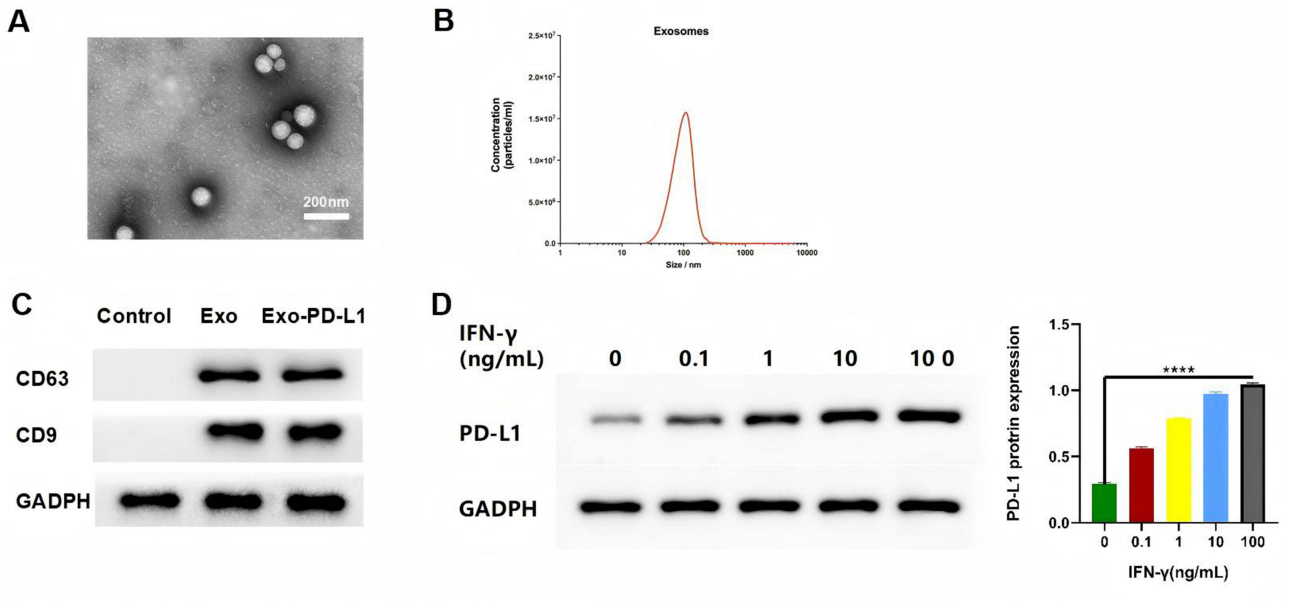

Figure 3 Characterization of exosomes. (**A**) TEM images of MSC exosomes; scale bar = 200 nm; (**B**) distribution of MSC exosomes; (**C**) specific proteins of MSC exosomes via WB analysis. (**D**) expression of PD-L1 via WB analysis. ****P<0.0001 vs control.

inflammatory factors (Figure 4C and D). These results indicated that Exo-PD-L1 can inhibit the activity of T cells and reduce the release of inflammatory factors.

Establishment of the CIA Model

We established a CIA model using DBA/1 mice following the experimental timeline outlined in Figure 5A. After a 1-week acclimatization period, mice were randomly assigned to four groups: Control, Saline, Exo, and Exo-PD-L1. Saline group with 0.1 mL saline; Exo group with 0.1 mL saline+1x10^7 particles/mL exosomes; Exo-PD-L1 group with 0.1 mL saline +1x10^7 particles/mL Exo-PD-L1. CIA modeling was performed on all groups except the Control group, with two immunizations administered on Day 0 and Day 7. Mice were monitored continuously, and CIA progression was scored as shown in Figure 5B. Post-modeling establishment, interventions were administered weekly via tail vein injection for 3 weeks. On Day 56, mice were euthanized for tissue collection. Compared with the blank group, the CIA scores of the Exo and Exo-PD-L1 groups decreased significantly after the intervention. As shown in Figure 5, the CIA score of the Exo-PD-L1 group decreased more significantly than that of the Exo group, whereas the CIA score of the saline group continued to increase. This indicates that the Exo-PD-L1 group had the most obvious effect on CIA score reduction (Figure 5).

Distribution of Exo-PD-L1 in Mice

Exo-PD-L1 and Exo were labeled with DiR. Mice with CIA of the same severity were divided into four groups: saline, DiR, DiR-labelled Exo, and DiR-labelled Exo-PD-L1. In vitro imaging was performed 2, 4, 6, 8, 12, and 24 h after injection. We observed almost no fluorescence in the saline group, and the fluorescence intensity in the DiR group was not obvious and was widely dispersed throughout the body of the mice. The fluorescence intensity and targeted aggregation of the Exo group were lower than those of the Exo-PD-L1 group were. This indicated that Exo-PD-L1 had a better targeting effect on joint inflammation than the other groups (Figure 6A). The mouse model used in this study mainly showed inflammation of the toe joint, whereas the control group consisted of healthy mice without inflammation. The organ distribution further showed that Exo-PD-L1 had a significant targeting ability to the inflamed joint site compared to the other groups (Figure 6B).

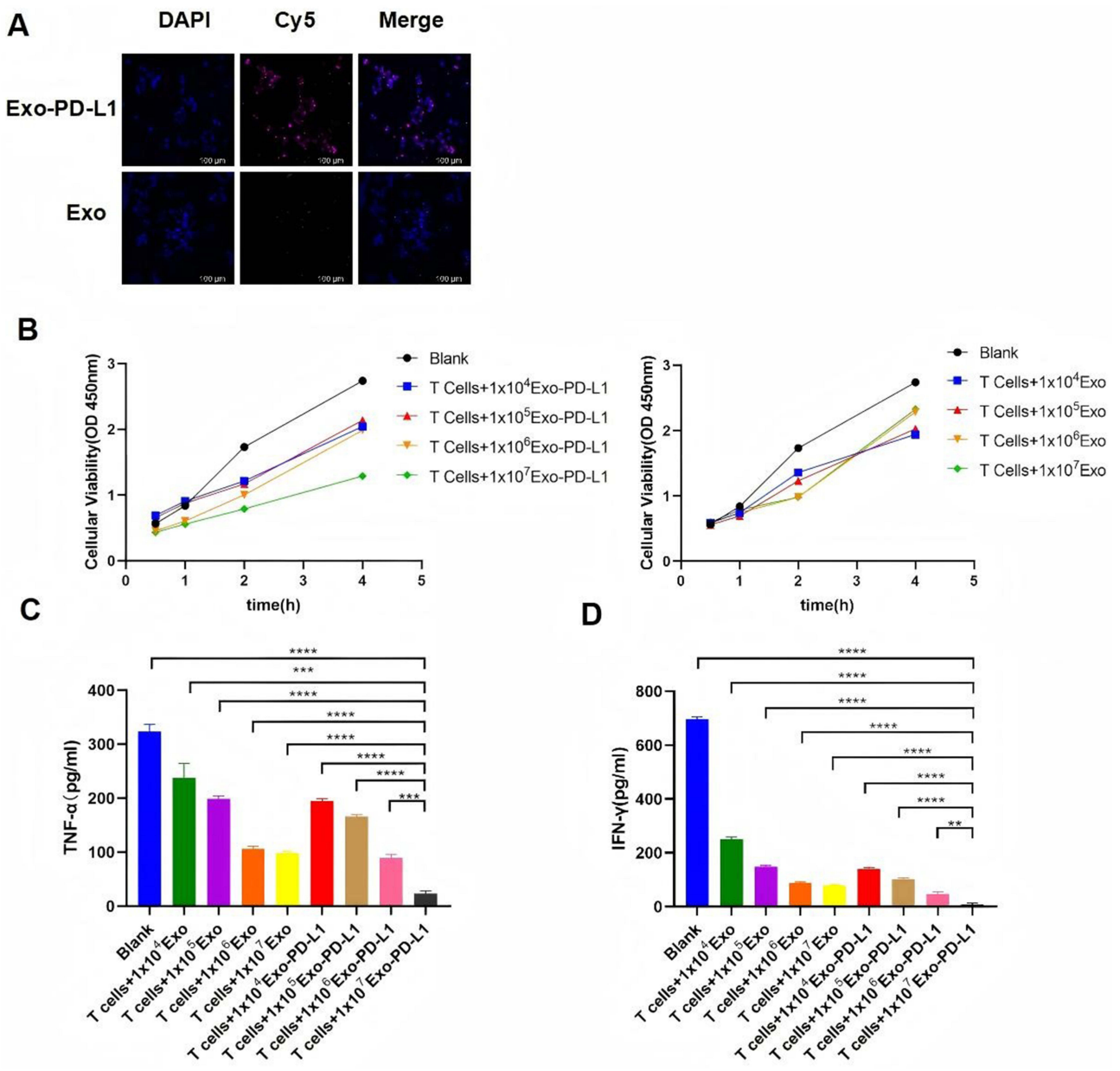

Figure 4 (**A**) Co-culture of Exo-PD-L1 with T cells. The interaction between exosomes and T cells was observed using fluorescence microscopy. (**B**) CCK-8 assay was used to detect the effect of different concentrations of Exo-PD-L1 on T cells. (**C** and **D**) Expression levels of proinflammatory cytokines TNF-α and IFN-γ in co-culture supernatants. ***P*<0.01, ****P*<0.001, *****P*<0.0001 vs control.

Therapeutic Effect of Exo-PD-L1 on CIA Model Mice

CIA model mice were photographed weekly and inflammation was observed in the toes of the limbs (Figure 7A). We found that the paw of mice in each model group was obviously swollen on day 42. After treatment which the swelling in the saline group was not significantly relieved, while the swelling in the Exo and Exo-PD-L1 groups was significantly reduced and subsided, and the effect of the Exo-PD-L1 group was more obvious. After 3 weeks of treatment, the mice were sacrificed, and the distal tibia of the right hind limb, ankle joint, and paw were harvested for micro-CT scanning and 3D reconstruction after removing excess soft tissue (Figure 7B). Obvious bone destruction was observed in the ankle and toe joints of the saline group. The Exo group had a better therapeutic effect, but the mice still showed a mild degree of bone destruction, which was significantly relieved in the Exo-PD-L1 group. Representative 3D reconstructed images of the hind paw obtained by micro-CT analysis showing bone degeneration (red arrows).

https://doi.org/10.2147/IJN.S522245

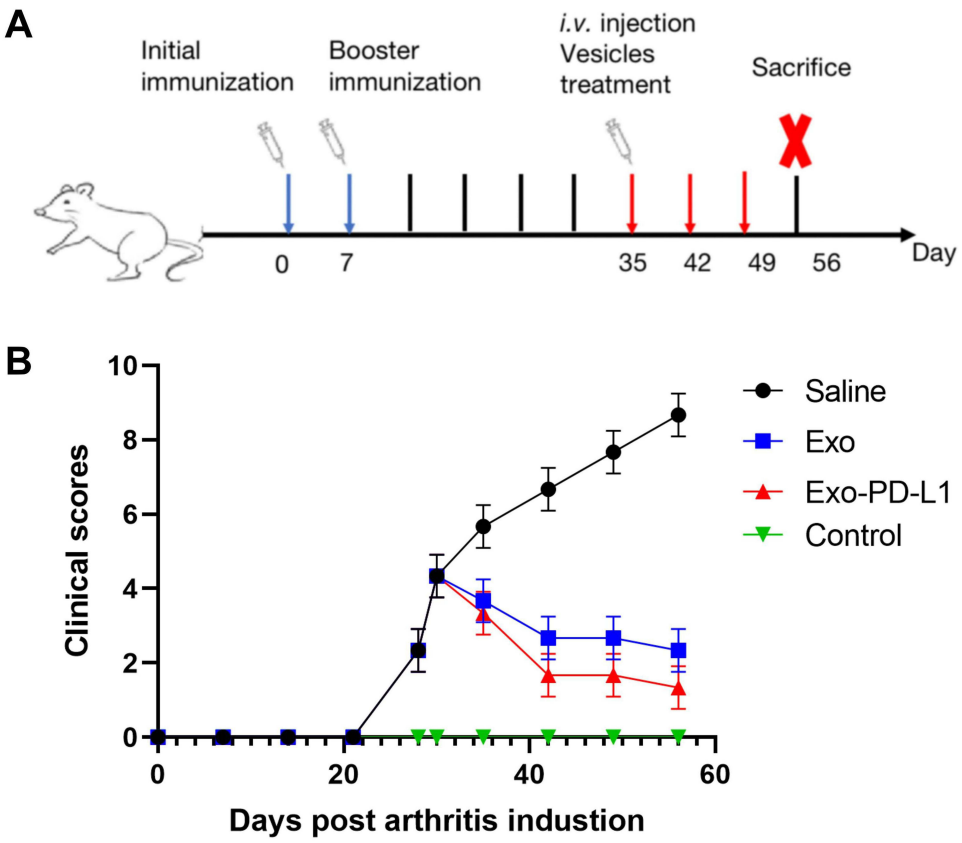

Figure 5 (**A**) Scheme of CIA model mice development and therapy. (**B**) CIA scores of the mice in each group.

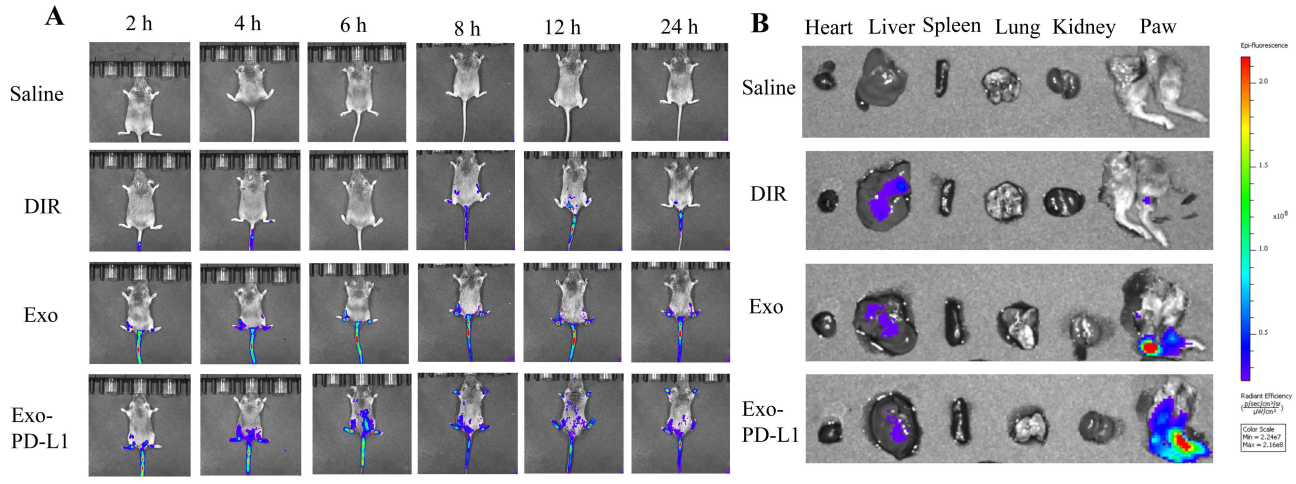

Figure 6 Biodistribution of exosomes in vivo. (**A**) In vivo imaging at 2, 4, 6, 8, 12, and 24 h. (**B**) Distribution of Saline, DIR, Exo and Exo-PD-L1 in different organs.

Synovial tissues were collected, and paraffin sections were prepared for histological observation. As shown in Figure 7C, HE staining showed that the synovial cells in the control group were evenly distributed and arranged regularly, whereas the synovial lining cells in the saline group were significantly abnormal, with a large number of inflammatory cells infiltrating the tissue and obvious bone destruction. Proliferation of lining cells in the Exo group was

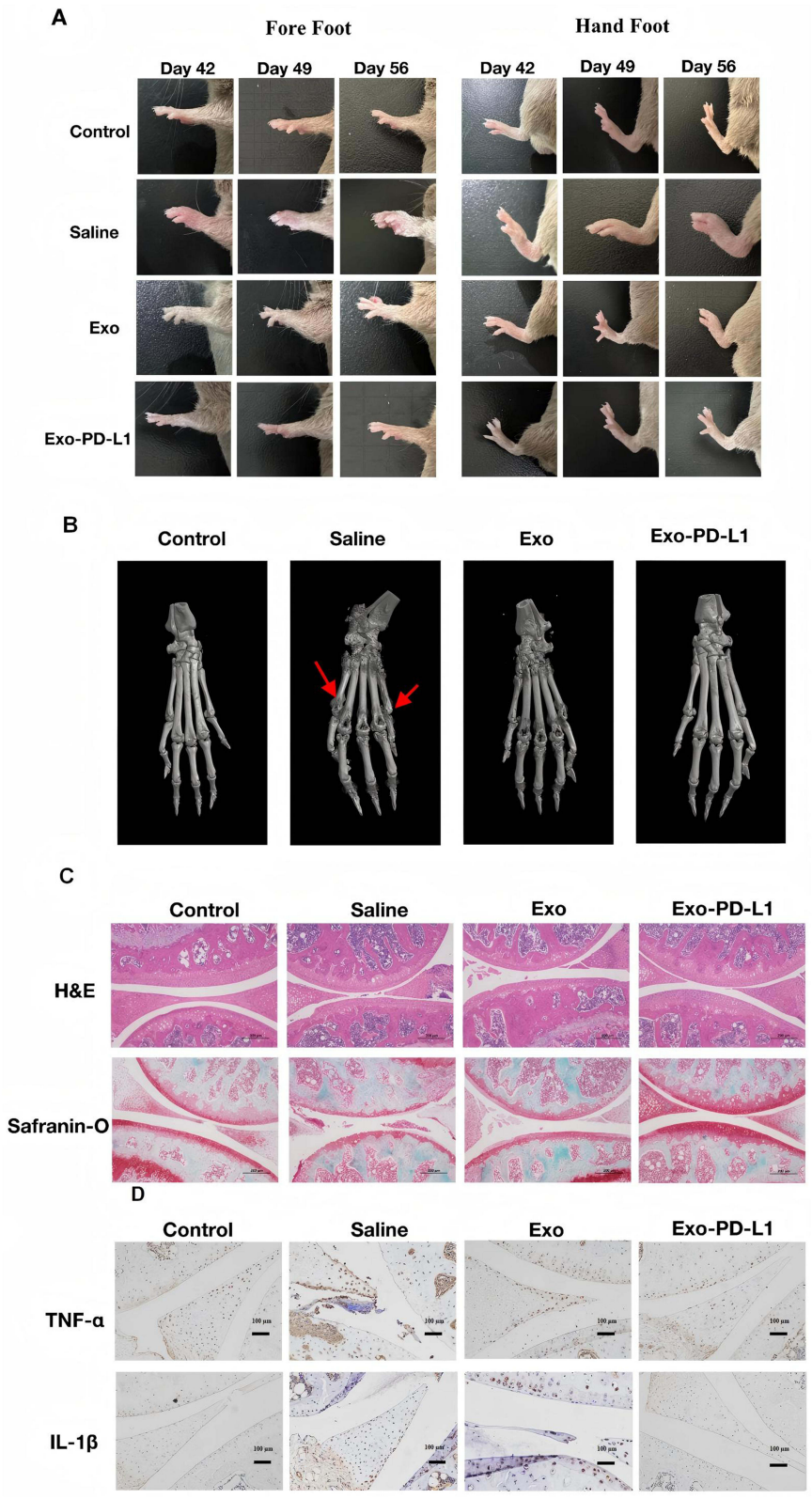

Figure 7 Treatment effects in CIA mouse models (**A**) Paw swelling of mice in each group; (**B**) 3D reconstruction of the foot and ankle was observed by micro-CT; (**C**) Representative images of H&E staining and safranin-fast green staining (scale bar, 200 μm); (**D**) The relative expression of TNF-α and IL-1β in synovial tissue of arthritis was determined by immunohistochemistry (scale bar, 200 μm).

https://doi.org/10.2147/IJN.S522245

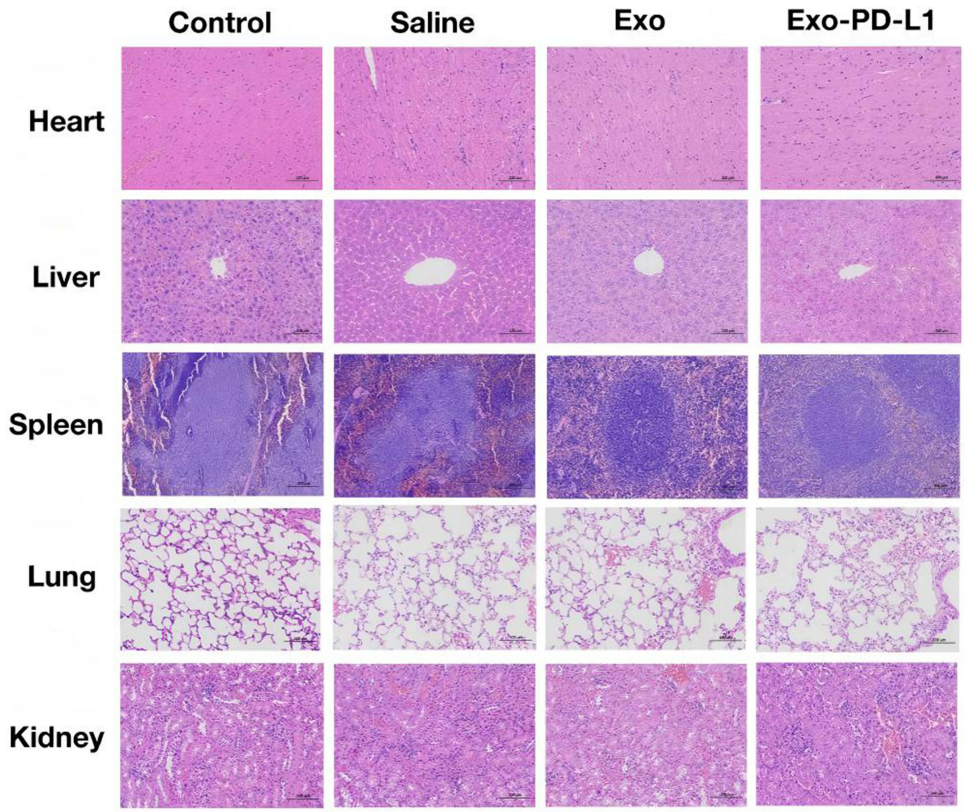

Figure 8 Biosafety Evaluation. HE-stained sections of major organs (heart, liver, spleen, lung, and kidney) from mice in each experimental group. Scale bar = 200 μm.

reduced, synovial hyperplasia was improved in the Exo-PD-L1 group, and inflammatory cell infiltration was not observed. Safranin and solid green staining (Safranin-O) showed that the cartilage surface of the control group was complete and the synovial cells were evenly distributed in the articular cavity. The cartilage surface in the saline group was interrupted and incomplete, the cartilage was obviously eroded and destroyed, and synovial hyperplasia was evident. The cartilage surface of Exo-PD-L1 was smooth and intact without erosion, and the synovial cells were evenly distributed without proliferation, indicating that Exo-PD-L1 could significantly reduce cartilage destruction in CIA mice, and that the protective effect of Exo-PD-L1 on bone damage was significantly better than that of Exo treatment (Figure 7C). Immunohistochemical staining showed that the expression of TNF-α and IL-1β in the synovium of the saline group was significantly increased compared with that in the control group, while in the Exo group, it was decreased, and in the Exo-PD-L1 group, it was almost absent.

Biological Safety Assessment of Exo-PD-L1

To evaluate the biological safety of MSCs, histological examinations were conducted on the major organs (including heart, liver, spleen, lung, and kidney) of CIA mice after they were treated with Saline, Exo, and Exo-PD-L1. Normal mice served as the Control group. HE staining showed that there were no obvious pathological changes in the organs of mice in the Exo and Exo-PD-L1 groups (Figure 8).

Discussion

MSC can inhibit the activation of T cells and change the phenotype of macrophages and dendritic cells, so it has the effect of immunosuppression.[10] Therefore, in this study, we used MSC for the cell experiments. We used IFN-γ to stimulate MSC to highly express PD-L1, extracted exosomes from Exo-PD-L1, and co-cultured Exo-PD-L1 with T-cells. We demonstrated that Exo-PD-L1 can be taken up by T cells and that Exo-PD-L1 can inhibit the activity of T cells cultured in vitro. Thus, the release of inflammatory factors from T cells was inhibited. Exo-PD-L1 was injected into the

blood of CIA, and it was observed that exosomes accumulated in inflamed joints. After a certain period, the arthritis manifestations and histological morphology of CIA mice were significantly improved compared to those of the control group. These results demonstrated the potential clinical utility of exosomes with high PD-L1 expression. The therapeutic mechanism of Exo-PD-L1 was illustrated in Scheme 1.

All the biomaterials used in this study underwent a process from exploration to confirmation. The isolated MSCs expressed CD44 and CD105 but not CD11b, CD45, or MHC II, which is consistent with the characteristics of MSCs. The purity of the isolated MSCs was 96.5%. Exosomes extracted by ultracentrifugation were verified by transmission electron microscopy, nanoparticle tracking analysis, and Western blotting. Therefore, these materials were reliable tools for this study.

We demonstrated that IFN-γ stimulated higher expression of PD-L1 in MSCs in a dose-dependent manner, and the amount of PD-L1 in exosomes produced by stimulated MSCs was also higher than that produced by wild-type MSCs (approximately 4-fold increase). MSCs had a good homing effect at inflammatory sites. The main mechanism was thought to be that inflammatory cells expressed a variety of chemokines, MSCs express a variety of chemokine ligands, and the migration of MSCs across endothelial cells was primarily affected by the concentration of chemokines. For example, chemokines CXCL12, CXCL8, CXCL4, CCL2, and CCL7 expressed by inflammatory cells activated their corresponding ligands on MSCs, leading to the trans-endothelial accumulation of MSCs at the sites of inflammation. Furthermore, CXCL12 was released from fibroblasts at the sites of inflammation in rats. Through ligand-receptor interactions, MSCs aggregation at inflammatory sites was strongly promoted.[19,20] Exosomes were hypothesized to inherit the homing ability of parent MSCs,[21] and we proposed that Exo-PD-L1 might retain homing properties through surface chemokine receptors[22.] However, direct evidence for exosome-specific homing mechanisms remained unvalidated and required further investigation. Although Exo-PD-L1 demonstrated potential for targeted immunosuppression, key challenges included: (1) potential immunogenicity of allogeneic exosomes, which could trigger host immune clearance; (2) difficulties in scalable exosome production with consistent PD-L1 loading; and (3) heterogeneity in inflammatory signaling across human diseases, which might compromise homing efficiency.[23] Clinical translation would require optimized exosome isolation protocols and preclinical validation in humanized models.

This study found that the fluorescence in the DIR + Exo group (the control group) also aggregated at the arthritis site, but the overall fluorescence intensity and targeted aggregation were lower than those in the DIR + EXO-PD-L1 group, suggesting that the expression of PD-L1 can promote the homing of exosomes to the inflammatory site, and the mechanism needs to be further studied. We speculated that PD1 is also a chemotactic factor.

Some novel approaches for treating RA emerged recently. Zhang et al[24] have demonstrated the efficacy of locally administered liposomal drug depots for sustained anti-inflammatory effects and cartilage repair through macrophage repolarization. Wu et al[25] synthesized a biocompatible multi-functional F-PCP nano-platform which integrates in situ O_2 generation/CDT/PTT, this nano-platform gathered to the inflammatory site of CIA mice, and inhibited the proliferation of M_1 macrophages which are also pathogenic cells, finally the bone erosion of the mice was eliminated. Additionally, engineered M2 macrophage-derived nanocomplexes have shown the ability to induce antigen-specific immune tolerance via cuproptosis-mediated elimination of activated T cells and amplification of TGF-β/Treg pathway.[26] Although the above approaches have their own advantages for RA treatment, MSC and MSC–derived exosomes can be harvested from the patient's own body, and have multiple pathways to block RA progression, both MSC and MSC-derived exosomes are still the candidates for the treatment for RA, for example, recently Bruckner et al[27] injected the human gingival-derived mesenchymal stem cells (GMSC) and GMSC-derived exosomes (GMSCEx) into chimeric humanized RA model mice, although the cells and exosomes were not modified, found that GMSC and GMSCEx can significantly inhibit the direct deleterious effects of synovial fibroblasts (RASF) on cartilage in this model and block the invasive migration of the RASF, which proved that the MSC and MSC-derived exosomes can act on RASF. Our Exo-PD-L1 strategy directly suppressed pathogenic T cell activation via PD-1/PD-L1 pathway, which adds a mechanism for MSC-based RA treatment. However, our study had some limitations: (1) The immunogenicity of allogeneic exosomes remains a critical translational barrier, as host immune responses against donor-derived exosomes may compromise therapeutic efficacy in clinical settings. (2) Scalable production under Good Manufacturing Practice standards requires further optimization to ensure batch-to-batch consistency in PD-L1 loading and exosome yield. (3) While Exo-PD-L1 demonstrated joint-targeting capacity in CIA models, its clinical relevance hinges on validating targeting efficiency in clinical

patients. (4) The IFN-γ concentration optimization was incomplete as only 100 ng/mL was validated; systematic dose-ranging studies are needed. (5) The cytokine analysis was relatively narrow, expanded panels covering Th1/Th17-related factors and detailed T-cell phenotyping would strengthen the findings.

Conclusion

To explore a novel therapeutic approach targeting T cells which are in the joints of RA, we successfully obtained exosomes derived from MSCs with Exo-PD-L1 through IFN-γ stimulation to MSCs. The Exo-PD-L1 could inhibit T cell activity in vitro, selectively accumulate in inflamed joints, and ameliorate synovitis and bone erosion without organ toxicity in CIA model mice. Therefore, our research demonstrated that Exo-PD-L1, as a novel, targeted, efficient, and safe therapeutic approach, has promising therapeutic potential for clinical translation in RA. Future studies will focus on long-term safety evaluation of Exo-PD-L1 in immunocompetent models and scalable production methods to ensure batch-to-batch consistency.

Data Sharing Statement

The datasets used and analyzed during the current study are available from the corresponding author on reasonable request.

Author Contributions

All authors made a significant contribution to the work reported, whether that is in the conception, study design, execution, acquisition of data, analysis and interpretation, or in all these areas; took part in drafting, revising or critically reviewing the article; gave final approval of the version to be published; have agreed on the journal to which the article has been submitted; and agree to be accountable for all aspects of the work.

Funding

The authors appreciate financial supports from the Jiangsu Province Postdoctoral Research Funding Program (2021K593C).

Disclosure

The authors declare that they have no known competing financial interests or personal relationships that could have appeared to influence the work reported in this paper.

References

1. Mitragotri S, Yoo J-W. Designing micro- and nano-particles for treating rheumatoid arthritis. *Arch Pharmacal Res*. 2011;34(11):1887–1897. doi:10.1007/s12272-011-1109-9
2. Firestein GS. Evolving concepts of rheumatoid arthritis. *Nature*. 2003;423(6937):356–361. doi:10.1038/nature01661
3. Alivernini S, Firestein GS, McInnes IB. Pathogenesis of. *Immunity*. 2022;55(12):2255–2270. doi:10.1016/j.immuni.2022.11.009
4. Choy EH, Panayi GS. Cytokine pathways and joint inflammation in rheumatoid arthritis. *N Engl J Med*. 2001;344(12):907–916. doi:10.1056/NEJM200103223441207
5. Smolen JS, Aletaha D, Koeller M, et al. New therapies for rheumatoid arthritis. *Lancet*. 2007;370(9602):1861–1874. doi:10.1016/S0140-6736(07)60784-3
6. Zheng X, Yang H, Zhang Z, et al. pH-responsive size-adjustable liposomes induce apoptosis of fibroblasts and macrophages for rheumatoid arthritis treatment. *Acta Biomater*. 2024;179:256–271. doi:10.1016/j.actbio.2024.03.006
7. Taylor PC, Moore A, Vasilescu R, et al. A structured literature review of the burden of illness and unmet needs in patients with rheumatoid arthritis: a current perspective. *Rheumatol Int*. 2016;36(5):685–695. doi:10.1007/s00296-015-3415-x
8. Chemin K, Gerstner C, Malmstrom V. Effector functions of CD4+ T cells at the site of local autoimmune inflammation lessons from Rheumatoid Arthritis. *Front Immunol*. 2019;10:353. doi:10.3389/fimmu.2019.00353
9. Li S, Yin H, Zhang K, et al. Effector T helper cell populations are elevated in the bone marrow of patients with rheumatoid arthritis and correlate with disease severity. *Sci Rep*. 2017;7(1):4776. doi:10.1038/s41598-017-05014-8
10. Luque-Campos N, Contreras-Lopez RA, Jose Paredes-Martinez M, et al. Mesenchymal stem cells improve rheumatoid arthritis progression by controlling memory T cell responses. *Front Immunol*. 2019;10:798. doi:10.3389/fimmu.2019.00798
11. Koliaraki V, Prados A, Armaka M, et al. Mesenchymal context in inflammation, immunity, and cancer. *Nat Immunol*. 2020;21(9):974–982. doi:10.1038/s41590-020-0741-2

12. Roh KH. Artificial methods for T Cell activation: critical tools in T cell biology and T Cell immunotherapy. *Adv Exp Med Biol*. 2018;1064:207–219.
13. Ponte AL, Marais E, Gallay N, et al. In vitro migration capacity of human bone marrow mesenchymal stem cells: comparison of chemokine and growth factor chemotactic activities. *Stem Cells*. 2007;25(7):1737–1745. doi:10.1634/stemcells.2007-0054
14. Wei W, Ao Q, Wang X, et al. Mesenchymal stem cell-derived exosomes: a promising biological tool in nanomedicine. *Front Pharmacol*. 2020;11:590470. doi:10.3389/fphar.2020.590470
15. Lin DY, Tanaka Y, Iwasaki M, et al. The PD-1/PD-L1 complex resembles the antigen-binding Fv domains of antibodies and T cell receptors. *Proc Natl Acad Sci U S A*. 2008;105(8):3011–3016. doi:10.1073/pnas.0712278105
16. Wei H, Chen F, Chen J, et al. Mesenchymal stem cell-derived exosomes as nanodrug carriers of doxorubicin for targeted osteosarcoma therapy via the SDF1-CXCR4 axis. *Int J Nanomed*. 2022;17:3483–3495. doi:10.2147/IJN.S372851
17. You G, Lim GT, Kwon S, et al. Metabolically engineered stem cell–derived exosomes regulate macrophage heterogeneity in. *Sci Adv*. 2021;7(23). doi:10.1126/sciadv.abe0083.
18. Chen G, Huang AC, Zhang W, et al. Exosomal PD-L1 contributes to immunosuppression and is associated with the anti-PD-1 response. *Nature*. 2018;560(7718):382. doi:10.1038/s41586-018-0392-8
19. Shin MJ, Park JY, Lee DH, et al. Stem cell-mimicking nanoencapsulation for targeting arthritis. *Int J Nanomed*. 2021;16:8485–8507. doi:10.2147/IJN.S334298
20. Wang S, Lei B, Zhang E, et al. Targeted therapy for inflammatory diseases with mesenchymal stem cells and their derived exosomes: from basic to clinics. *Int J Nanome*. 2022;17:1757–1781. doi:10.2147/IJN.S355366
21. Beyth S, Borovsky Z, Mevorach D, et al. Human mesenchymal stem cells alter antigen-presenting cell maturation and induce T-cell unresponsiveness. *Blood*. 2005;105(5):2214–2219. doi:10.1182/blood-2004-07-2921
22. Phinney DG, Pittenger MF. Concise review: MSC-derived exosomes for cell-free therapy. *Stem Cells*. 2017;35(4):851–858. doi:10.1002/stem.2575
23. Campbell CR, Berman AE, Weintraub NL, et al. Electrical stimulation to optimize cardioprotective exosomes from cardiac stem cells. *Med Hypotheses*. 2016;88:6–9. doi:10.1016/j.mehy.2015.12.022
24. Zhang Z, Wang G, Zhang Z, et al. Locally administered liposomal drug depot enhances rheumatoid arthritis treatment by inhibiting inflammation and promoting cartilage repair. *J Nanobiotechnol*. 2025;23(1):1.
25. Wu X, Gao G, Chen H, et al. Fenton/Fenton-like microreactor in inflammatory microenvironment: photothermal enhanced catalytic oxidation strategy for chemodynamic treatment of rheumatoid arthritis. *Chem Eng J*. 2023;474(145765):1–13. doi:10.1016/j.cej.2023.145765
26. Wu G, Su T, Zhou P, et al. Engineering M2 macrophage-derived exosomes modulate activated T cell cuproptosis to promote immune tolerance in rheumatoid arthritis. *Biomaterials*. 2025;2025:315.
27. Bruckner S, Capria VM, Zeno B, et al. The therapeutic effects of gingival mesenchymal stem cells and their exosomes in a chimeric model of rheumatoid arthritis. *Arthritis Res Ther*. 2023;25(1):211–222. doi:10.1186/s13075-023-03185-6